Developmental Cell
Article

The Extracellular Domain of Notch2 Increases Its Cell-Surface Abundance and Ligand Responsiveness during Kidney Development

Zhenyi Liu,[1] Shuang Chen,[1] Scott Boyle,[1] Yu Zhu,[1] Andrew Zhang,[1] David R. Piwnica-Worms,[1,2,3] Ma. Xenia G. Ilagan,[1] and Raphael Kopan[1,4,5,*]
[1]Department of Developmental Biology
[2]Molecular Imaging Center, Mallinckrodt Institute of Radiology
[3]BRIGHT Institute
[4]Division of Dermatology, Department of Medicine
Washington University School of Medicine, 660 South Euclid Avenue, St. Louis, MO 63110, USA
[5]Present address: Division of Developmental Biology, Cincinnati Children's Research Foundation, 3333 Burnet Avenue, ML 7007, Cincinnati, OH 45229, USA
*Correspondence: rafi.kopan@gmail.com
http://dx.doi.org/10.1016/j.devcel.2013.05.022

SUMMARY

Notch2, but not Notch1, plays indispensable roles in kidney organogenesis, and Notch2 haploinsufficiency is associated with Alagille syndrome. We proposed that proximal nephron fates are regulated by a threshold that requires nearly all available free Notch intracellular domains (NICDs) but could not identify the mechanism that explains why Notch2 (N2) is more important than Notch1 (N1). By generating mice that swap their ICDs, we establish that the overall protein concentration, expression domain, or ICD amino acid composition does not account for the differential requirement of these receptors. Instead, we find that the N2 extracellular domain (NECD) increases Notch protein localization to the cell surface during kidney development and is cleaved more efficiently upon ligand binding. This context-specific asymmetry in NICD release efficiency is further enhanced by Fringe. Our results indicate that an elevated N1 surface level could compensate for the loss of N2 signal in specific cell contexts.

INTRODUCTION

The kidney is an essential organ with growing clinical importance in the aging western population. It regulates excretion of soluble waste, maintains pH and electrolyte balance, and controls blood pressure and vitamin D levels. Its functional unit, the nephron, consists of a filtration apparatus called the glomerulus, followed by renal tubules made up of specialized epithelial cells that modify the filtrate, which eventually flows into the collecting duct system and drains into the bladder.

During development, nephrons form as the outcome of reciprocal interactions between the metanephric mesenchyme (MM) and the ureteric bud (UB) (Costantini and Kopan, 2010). Gonadal-derived neurotrophic factor (GDNF), secreted by the MM, induces UB branching; Wnt9b, secreted by the UB, induces a few MM cells to undergo mesenchymal to epithelial transition (MET) and form a renal vesicle (RV), which grows into the S-shaped body (SSB) after fusing with the ureteric stalk (Figure 1A; Georgas et al., 2009). Together with endothelial and mesangial cells, the proximal third of the SSB forms the glomerulus; the rest of the SSB gives rise to the various segments and cell types that link the glomerulus to the collecting duct.

In both human and mouse, proper renal organogenesis requires the Notch signaling pathway. This pathway is comprised of four Notch receptors (N1–N4) and five canonical ligands (Dll1, Dll3, Dll4, Jag1, and Jag2; Kopan and Ilagan, 2009). As all receptors and ligands are type I transmembrane proteins, the Notch pathway mediates communications between adjacent cells. Binding of the ligand to the Notch extracellular domain (NECD) exposes the S2 cleavage site, which by default is masked by the negative regulation region (NRR). Cleavage at the S2 site is followed by intramembrane proteolysis at the S3 site by γ-secretase, which releases the Notch intracellular domain (NICD) from the cell membrane. Subsequently, NICD translocates to the nucleus and forms a transcriptional activation complex with RBP and Mastermind on specific DNA sites to turn on the expression of target genes, including Hes/Hey family members. In addition to these core pathway components, various other factors can modulate the strength of the Notch signaling pathway (Kopan and Ilagan, 2009).

Despite the presence of N1, N2, Dll1, and Jag1 in the developing nephron, only haploinsufficiency in either *JAG1* or *N2* causes Alagille syndrome in humans, a disease characterized by craniofacial abnormalities and heart, liver, and kidney malformations (Penton et al., 2012). McCright et al. (2002) showed that in order to model Alagille syndrome in mice, simultaneous reduction of both *N2* and *Jag1* is required. Moreover, Cheng et al. (2007) reported that whereas removal of *N1* from the nephron progenitors was well tolerated, conditionally removing *N2* alone from nephron progenitors in the intermediate mesoderm (with *Pax3-Cre*) resulted in complete loss of the proximal nephron and the death of newborn pups within 48 hr. In another study, the contribution of *N1* could only be revealed in a sensitized

genetic background in which *N2* levels were reduced (Surendran et al., 2010). Thus far, a molecular explanation for the unequal role of *N2* (versus *N1*) and *JAG1* (versus other ligands) in human and mouse kidney development and disease has remained elusive.

To address this question, we used multiple approaches to determine whether differences in the spatial expression domains, the expression level, or the amino acid composition could account for the unequal contributions of N1 and N2 to nephron development. We demonstrated that the expression levels of N1 and N2 proteins are equivalent within the renal epithelia, and that differential expression outside of this domain did not contribute to the functional differences. To address the role of amino acid composition, we seamlessly swapped the entire N1ICD and N2ICD genomic coding regions to create two strains of mice harboring genes we call *N12* and *N21.* These mice provide a unique platform for distinguishing NICD dose-dependent phenomena from NICD composition-dependent ones in various tissues and disease models (Chu et al., 2011; Fan et al., 2004; Graziani et al., 2008; Parr et al., 2004; Rangarajan et al., 2001). Using these tools, we demonstrated that N1ICD and N2ICD are fully interchangeable during kidney development: nephrogenesis occurs normally in each of the 10,000 nephrons as long as N2ECD controls ICD release, but fails to complete any nephrons when N1ECD controls ICD release. This confirmed the existence of a threshold, a developmental switch that is controlled by the concentration, but not the composition, of Notch ICDs. The switch determines whether an individual nephron will develop its proximal elements (Cheng et al., 2007).

To gain more insight into how the ECD controls the free NICD concentration, we determined whether N1ECD and N2ECD differ in efficiency of ICD release in vitro using the Notch luciferase complementation imaging (LCI) assay (Ilagan et al., 2011). We show that when it is present at similar levels on the surface of HEK293 cells, N2ECD is consistently, but only marginally (~2-fold), better than N1ECD at releasing ICD in response to either Jag1 or Dll1. We further found that in RVs and SSB cells, N2 is more abundant on the cell surface than N1. Using N12 and N21 strains, we demonstrated that this uneven distribution is determined by the ECD. Finally, a series of ligand loss-of-function alleles revealed a dose-dependent effect for ligands and a dominant requirement for *Jag1* in the kidney context relative to that of Dll1. This may be amplified by ECD glycosylation by one of the three Fringe genes, Lunatic Fringe (Lfng), whose expression overlaps with N1 in the developing nephron. We propose that the combined effects of these factors make the N2 contribution critical for kidney development. The importance of the ECD in the kidney epithelial cell is also reflected in the labeling frequencies of N1::Cre^{LO} and N2::Cre^{LO} reporter mice (Liu et al., 2011; Morimoto et al., 2010; Vooijs et al., 2007), in which the release of Cre recombinase is solely determined by the Notch ECD. In summary, these data imply that the number of NICD molecules in the nucleus of RV cells is near the amount needed to promote proximal nephron development, which would explain why the loss of one *N2* or *Jag1* allele causes a developmental syndrome in humans. Because the ICDs are interchangeable, investigating N1 trafficking in organs affected by Alagille syndrome may lead to therapeutic benefit without the risk associated with agonist use.

RESULTS

N1 and N2 Have Similar Expression Patterns in Developing Renal Epithelia

We reasoned that the functional difference between the two Notch paralogs during metanephric kidney development could be explained by one mechanism or possibly a combination of several mechanisms, including (1) differences in promoters/enhancers, which give rise to differential temporal or spatial expression domains by controlling messenger RNA (mRNA) levels; (2) differences in the 3′ UTRs, which may affect the stability/translation of mRNAs of Notch paralogs and therefore protein abundance; (3) differences in ECD composition, which lead to differential responses to ligands and consequently different numbers of NICD molecules released, resulting in different signal "strengths"; and (4) differences in ICD composition, which lead to differential associations with distinct binding partners and activation of unique downstream targets (Spitz and Furlong, 2012).

Up to now, a careful examination of the N1 and N2 expression patterns in the developing kidney has not been possible due to the lack of appropriate antibodies. After confirming the specificity of newly developed antibodies against the N1ICD and the N2ICD (see below), we analyzed the expression patterns of these receptors at embryonic day 17.5 (E17.5) using immunofluorescence on wild-type (WT) kidneys (Figure 1). Both receptors are expressed in an overlapping cell population in the RV and SSB that is thought to give rise to proximal tubules and podocytes (Figures 1E–1L). In addition to the renal epithelia, N1 is expressed in endothelial precursor cells within the kidney anlagen (Figure 1B, arrowheads). In contrast, N2 is broadly expressed in the MM, vascular smooth muscle cells (VSMCs), and the UB, but is absent from endothelial cells (Figures 1C and 1D).

The exclusive expression of N2 in the MM may explain why this protein is indispensable (Fujimura et al., 2010). However, because progenitor maintenance and MET proceed normally in the absence of N2 (Cheng et al., 2007; McCright et al., 2002), N2 activation in MM is unlikely to perform a significant function there (Boyle et al., 2011). To directly test whether N2 is activated in MM cells, we examined the labeling pattern of an N2-activation-dependent reporter line, N2::Cre^{LO} (Figure S1 available online; Liu et al., 2011; Vooijs et al., 2007). In this reporter line, one copy of the N2ICD is replaced with Cre recombinase, which is released upon N2 activation. In the presence of the reporter allele Rosa$^{CAG\text{-}EYFP}$ (Madisen et al., 2010), the released Cre will excise the floxed "stop" cassette between the Rosa/CAG promoter and enhanced yellow fluorescent protein (EYFP) reporter and activate EYFP expression, indelibly marking cells that have experienced N2 activation (and their progeny; Vooijs et al., 2007). The N2::Cre^{LO} labeling pattern in E17.5 kidneys revealed only a few EYFP-positive cells in Six2-positive MM cells (Figures 1M and 1O). The few MM cells that experience N2 activation will most likely exit the stem cell niche (Boyle et al., 2011; Cheng et al., 2007; Fujimura et al., 2010). If N2 receptors were activated in cells undergoing MET, most RV cells would be labeled. Instead, only a few EYFP-positive cells are detected in RVs. Consistent with Notch activation in the RV, many labeled cells are seen in the SSBs, proximal tubules, and podocytes. N2 activation thus occurs in the

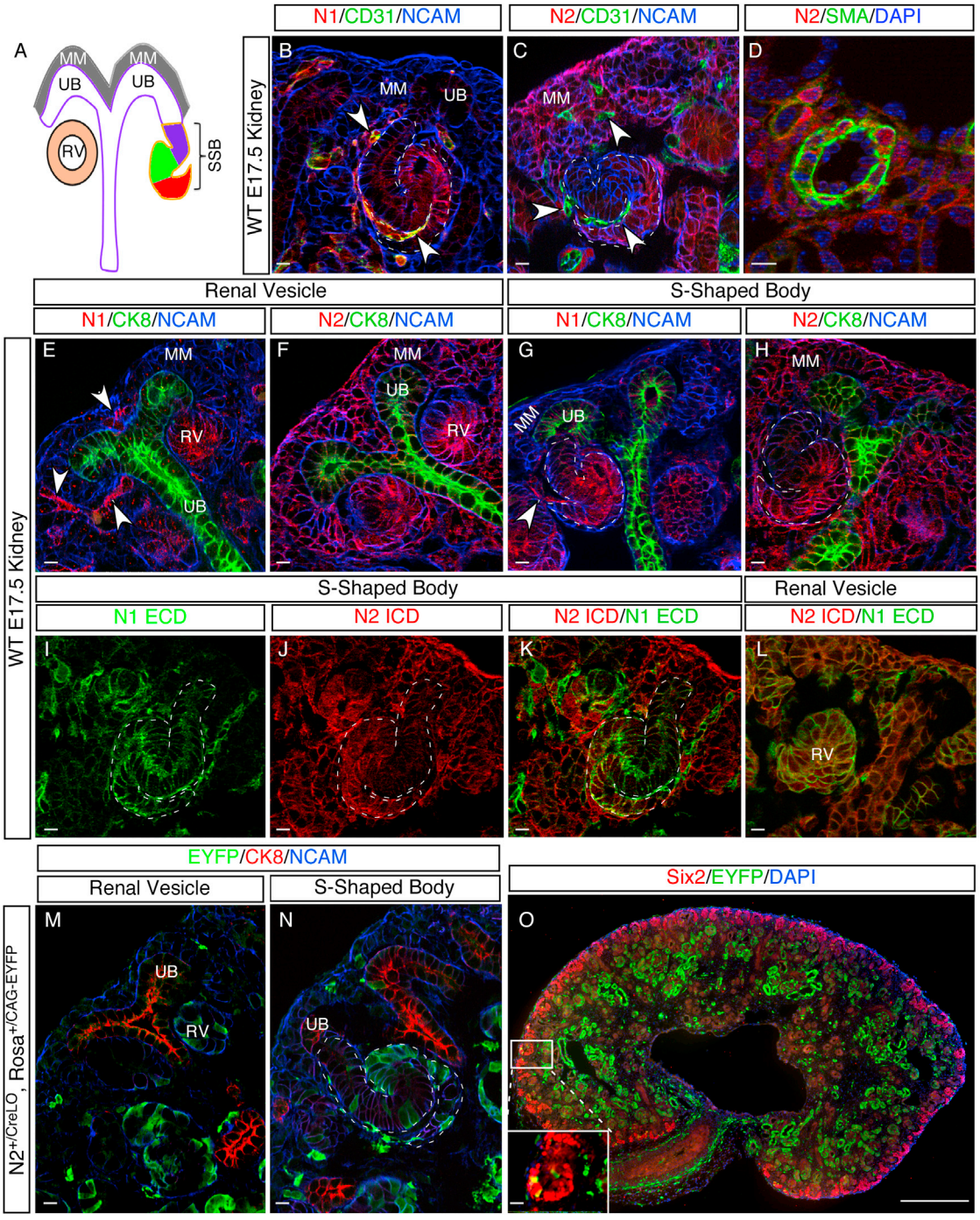

Figure 1. Variation in the Expression Pattern of N1 and N2 Does Not Explain Their Functional Difference

(A) Diagram showing major structures of developing nephrons. The presumptive distal and proximal tubules, as well as podocyte precursor cells, are denoted in purple, green, and red, respectively.

(B–L) Comparison of N1 and N2 expression in different structures of an E17.5 kidney. CD31 marks endothelial cells; smooth muscle actin (SMA) marks vascular smooth muscle cells; cytokeratin 8 (CK8) marks UB and its derivatives; neural cell adhesion molecule (NCAM) marks all epithelial cells. Arrowheads denote endothelial cell precursors.

(I–L) Double staining with N1ICD and N2ECD antibodies.

(M–O) Labeling pattern of N2::Cre reporter in E17.5 kidney. All scale bars are 10 μm except for (O), where it is 500 μm.

See also Figure S1.

epithelial cells and not in their mesenchymal precursors (Figures 1M–1O). In summary, both receptors are expressed in the domain where Notch proteins impact the decision to make proximal nephron cells, and the differential expression of N2 in the MM does not explain why N2 is essential for kidney development but N1 is not.

ICD Swap between N1 and N2 Creates N12 and N21 Chimeric Receptors

All NICD paralogs form transcriptional activation complexes with RBPjk and Mastermind on target promoters. Although Notch proteins can activate similar targets and can act redundantly in vivo (Riccio et al., 2008), in vitro and in vivo studies suggest that in some contexts, these complexes are distinct because NICD paralogs can have different or even opposite functions (Chu et al., 2011; Fan et al., 2004; Graziani et al., 2008; Parr et al., 2004; Rangarajan et al., 2001). Amino acids that are not conserved between N1ICD and N2ICD are located at the solvent-accessible surface of the Ankyrin domain and could therefore participate in unique interactions with putative coactivators or corepressors, contributing to their functional differences (Spitz and Furlong, 2012). To investigate this, we used galK-selection-based bacterial artificial chromosomes (BAC) recombineering (Warming et al., 2005) to swap the entire genomic regions coding the ICDs between the N1 and N2 loci in B6-derived embryonic stem cells (ESCs; Figure 2A; Figure S2). The swapped region ranged from exon 28, coding for the transmembrane domain (TMD), to the stop codon in exon 34. In order to retain transcript-specific regulation of mRNA stability and translation, we did not swap the 3′ UTRs. We designated the alleles *N12* (N2ICD in the N1 locus) and *N21* (N1ICD in the *N2* locus; Figure 2A). To facilitate ESC screening and postrecombination analysis with pyrosequencing-based methods (Liu et al., 2009, 2010), we introduced silent single nucleotide variations (SNVs) into the TMD coding regions (G38066C for *N12* and G125011C for *N21*), as well as an SNV in the ICD coding region of *N12* (G38129A; Figure 2A). After germline transmission was obtained, the *frt*-flanked neomycin/G418 selection cassette was removed by mating the mice with flippase deleter mice (Rodríguez et al., 2000). This left a 34 bp *frt* sequence between the stop codon and the 3′ UTR in mice with *N12* and *N21* chromosomes (Figure 2A; Figure S2).

PCR amplification confirmed the presence of the hybrid exon 28 in the genome (Figures S3A and S3B). Loss of sequences from *N1* exon 30 or *N2* exon 34, respectively, identified $N1^{12/12}$ and $N2^{21/21}$ homozygous mice, which are both viable (Figures S3A and S3B; a detailed phenotypic analysis of other organs will be described elsewhere). The loss of N1ICD in $N1^{12/12}$ or N2ICD in $N2^{21/21}$ mice was also confirmed by western blot with N1ICD- and N2ICD-specific antibodies, respectively (Figure 2B). The introduced SNVs allowed us to compare the mRNA levels transcribed from the *N12* chromosome to *N1* and the *N21* chromosome to *N2* in various heterozygous tissues of $N1^{+/12}$ and $N2^{+/21}$ mice, respectively, with pyrosequencing (Figure 2C). This analysis revealed that the shorter transcript was slightly more abundant in all tissues examined (Figure 2C). Western blot and immunostaining with either anti-Notch ICD or anti-Notch ECD antibody confirmed the expression of chimeric proteins (Figure 2B; Figures S3C and S3D). To assess whether the chimeric Notch receptors could reach the cell surface as efficiently as the endogenous receptors, we isolated RV and SSB cells from Lfng-GFP mice, in which EGFP is expressed under the control of LFng regulatory sequences. Double staining of E17.5 kidneys with either N1ICD or N2ICD antibodies showed an extensive overlap with EGFP (Figures 2D–2G; Figure S3E). To exclude the epithelial cells from differentiated tubules, we isolated GFP+ cells from E13.5, Lfng-GFP; $N1^{+/+}$; $N2^{+/+}$ (denoted as WT), Lfng-GFP; $N1^{12/12}$; $N2^{+/+}$ (denoted as $N1^{12/12}$) and Lfng-GFP; $N1^{+/+}$; $N2^{21/21}$ (denoted as $N2^{21/21}$) kidneys before tubule formation (Figure 3H), and stained them with anti-N1ECD- or anti-N2ECD-specific antibodies (Fiorini et al., 2009). Flow cytometry analysis confirmed that the cell-surface distribution of N12 and N21 was similar to that of N1 and N2, respectively (Figure 3I).

N1ICD and N2ICD Are Interchangeable in the Kidney

We previously showed that conditional deletion of N2 from the intermediate mesoderm (with *Pax3-Cre*) produced mice with nonfunctional, hypoplastic kidneys lacking podocytes and proximal tubules (Cheng et al., 2007). We found that $N2^{21/21}$ and compound heterozygous $N1^{+/-}$; $N2^{21/-}$ mice (both lacking N2ICD) formed functional nephrons in normal numbers (Figure 3). This result demonstrates that even a single copy of N1ICD can fully rescue the loss of N2ICD when expressed from the N2 locus. In contrast, when the endogenous *N2* alleles are conditionally deleted, even the presence of two copies of N2ICD expressed from the *N1* locus (*Pax3-Cre;* $N2^{f/f}$; $N1^{12/12}$) cannot rescue a single nephron (Figure 3). These mice were indistinguishable from *Pax3-Cre;* $N2^{f/f}$ mice in terms of kidney morphology and died within 24 hr of birth (Figure 3). These data demonstrate that N1ICD and N2ICD are fully interchangeable, and that the functional differences between N2 and N1 are determined by differences in their ECDs and/or their corresponding protein levels during kidney development.

N2 and *N1* Promoters/3′ UTRs Deliver Similar Levels of Protein in RV and SSB Cells

We next sought to determine whether N1 is less abundant than N2 protein within RVs and/or SSBs, which would explain the differences in their function during kidney development. This is a technically challenging question to answer, for two reasons: first, it proved impractical to isolate enough RV and SSB cells for western blot analysis; second, different antibodies that recognize unique epitopes in Notch paralogs may have different affinities, making the comparison difficult. Fortunately, the domain swap gave us the opportunity to examine N2ICD protein levels by immunostaining in WT (where N2ICD production is under the control of the endogenous *N2* locus) and *N12; N21* double-homozygous ($N1^{12/12}$; $N2^{21/21}$) mice (where all N2ICD production is under the control of the *N1* locus).

To perform this experiment, we first confirmed the specificity of the anti-N1ICD and anti-N2ICD antibodies on kidney sections from either $N1^{12/12}$ or $N2^{21/21}$ mice (Figures 4A and 4B). Next, we used the anti-N2ICD antibody and analyzed immunostained kidneys from $N2^{+/-}$, WT, and $N1^{12/12}$; $N2^{+/+}$ mice, which have one, two, and four copies of the N2ICD antigen, respectively (Figures S4A–S4C). Pixel intensity correlated well with gene dose (Figure S4D), confirming that this assay is sensitive enough

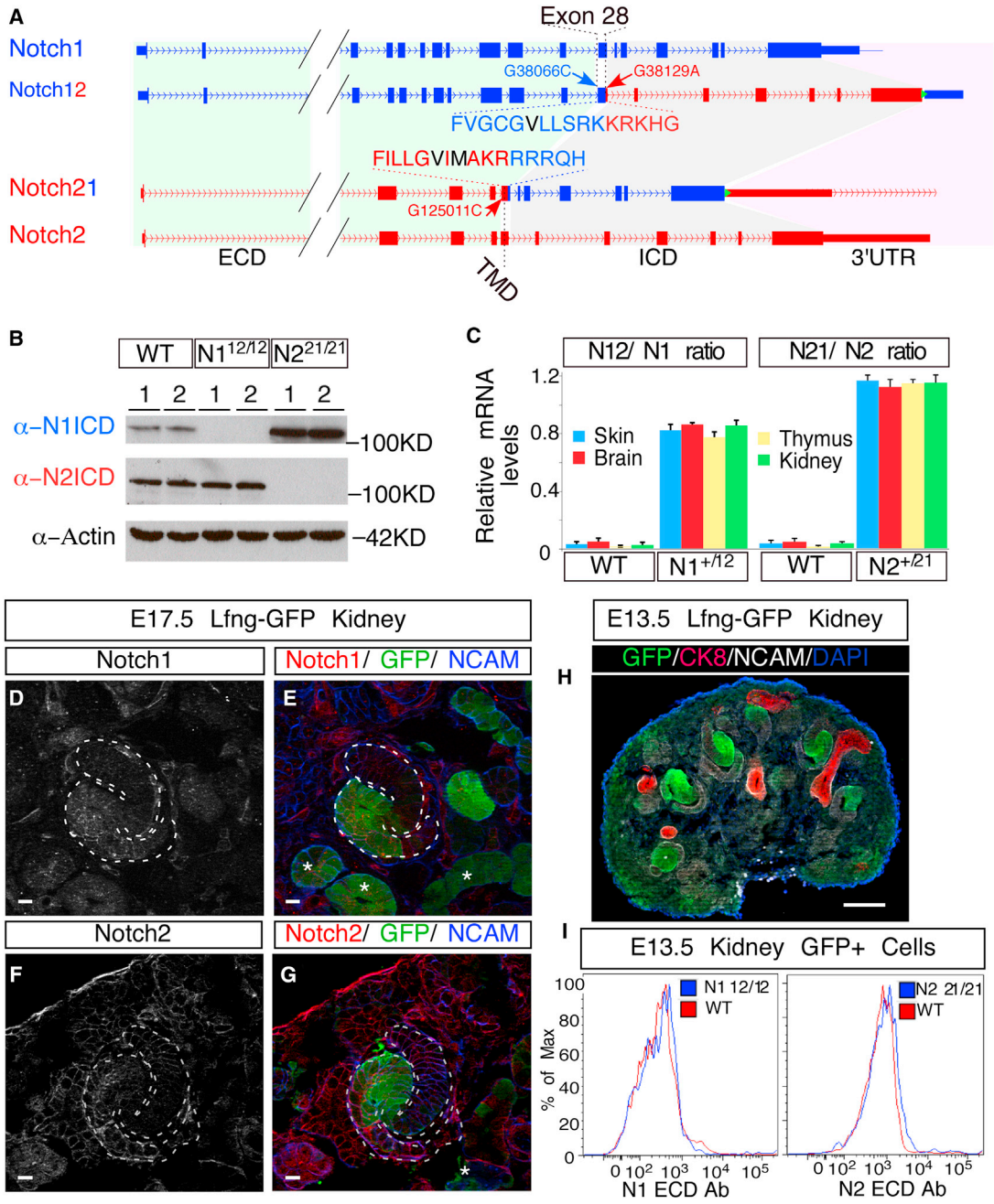

Figure 2. Generation of the N12 and N21 Alleles

(A) Schematic illustration of N1 (blue) and N2 (red) loci before and after the ICD swap. The N1ICD encompasses 5,926 bp on chromosome 2, ranging from nucleotide +38,103 to +44,028 (A in ATG is +1) and encoding amino acid 1,750 to 2,531; for *N2*, the ICD encompasses 8,699 bp on chromosome 3, ranging from nucleotide +125,048 to +133,746 and encoding amino acid 1,705 to 2,473. Amino acids in black denote the S3 cleavage sites. Green triangle denotes FRT site.

(B) Western blot analyses with ICD-specific antibodies of kidney extracts from newborn pups with designated genotypes (WT, $N1^{12/12}$, and $N2^{21/21}$; two different individuals per genotype).

(C) mRNA level comparisons between chimeric N12 and N21 and their corresponding endogenous alleles in various tissues of WT, $N1^{+/12}$, and $N2^{+/21}$ newborn pups. Allele ratios were calculated by determining the G/C ratio at SNVs G38066C and G125011C introduced into the targeting constructs with pyrosequencing. Error bars represent SD.

(D–G) Double staining of EGFP and N1 (D and E) or N2 (F and G) on E17.5 Lfng-GFP kidneys. Asterisks (*) denote EGFP+ tubules.

(H) EGFP labeling patterns in E13.5 Lfng-GFP kidney.

(I) E13.5 Lfng-GFP kidneys with WT or single homozygous ($N1^{12/12}$ or $N2^{21/21}$) Notch alleles were dissociated into single cells, stained with PE-conjugated N1ECD- or N2ECD-specific antibodies (eBioscience), and analyzed by flow cytometry. The cell-surface levels of WT (N1, N2) and chimeric (N12, N21) receptors were compared in EGFP+ cells. Scale bars: (D–G) 10 μm; (H) 100 μm.

See also Figures S2 and S3.

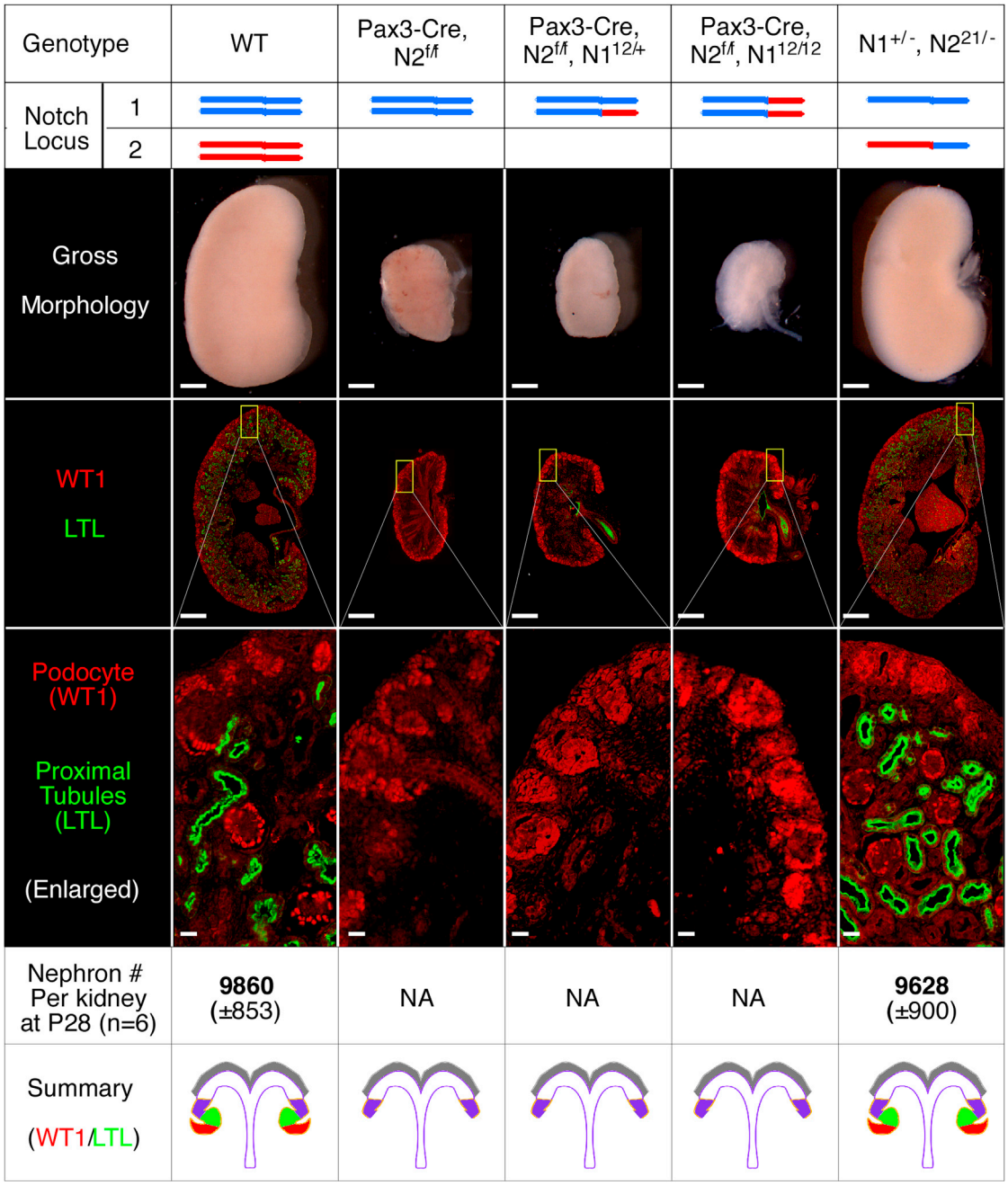

Figure 3. Notch ICDs Can Functionally Replace Each Other in Kidney Development

Kidney phenotypes were characterized in newborn mice with the indicated genotypes. Scale bars: 500 μm for whole kidneys, and 20 μm for the magnified windows showing WT1 and LTL staining. SDs of nephron number are shown in parentheses.

to quantitatively compare N2ICD levels in WT and $N1^{12/12}$; $N2^{21/21}$ mice. Finally, we compared the abundance of N2ICD protein levels in kidneys from WT and $N1^{12/12}$; $N2^{21/21}$ by immunostaining (Figure 4). Anti-N2ICD antibody staining of $N1^{12/12}$; $N2^{21/21}$ kidneys confirmed that N2ICD recapitulated the N1 expression pattern, including its strong expression in the developing RVs, SSBs, and all endothelial precursor cells, and its absence from the MM (Figures 4C and 4D). Importantly, the expression levels in RVs and SSBs were comparable in the two samples (Figures 4E and 4F). Therefore, the functional differences between N1 and N2 could not be attributed to differential expression levels, microRNA targeting of their 3′ UTRs, or their ICD composition.

Receptors Containing N2ECD Are More Abundant on the Plasma Membrane of RV and SSB Cells

Since only receptors on the cell surface could engage with ligands for activation, we sought to determine whether the

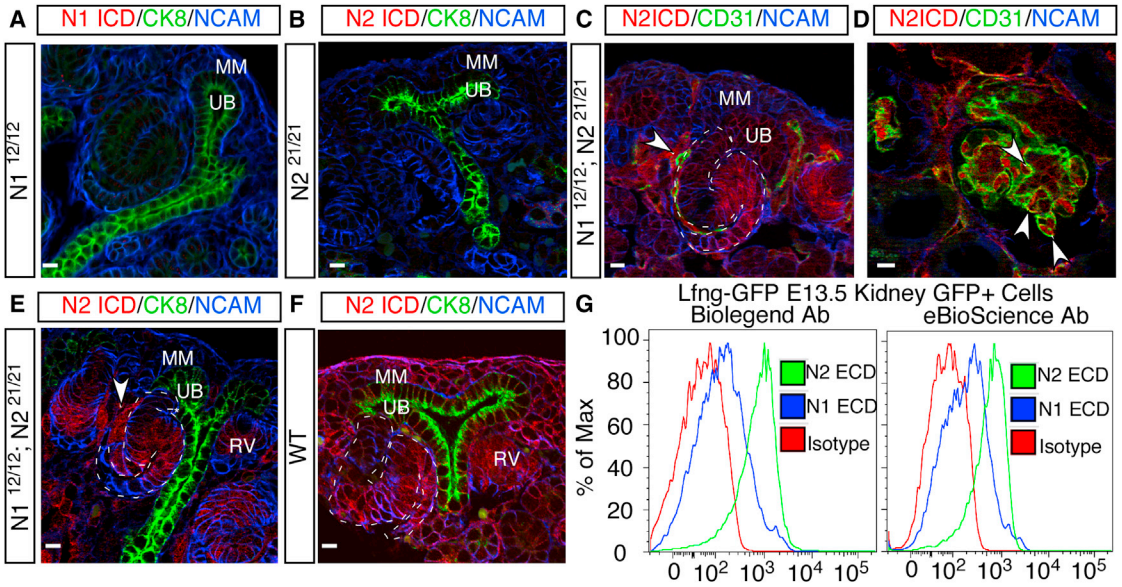

Figure 4. Comparison of the Total and Surface Levels of N1 and N2 in Developing Nephron Epithelia

(A and B) Confirmation of the specificity of anti-N1ICD and -N2ICD antibodies on kidney sections from $N1^{12/12}$ (A) and $N2^{21/21}$ (B) mice.

(C and D) Anti-N2ICD antibody staining on kidney sections from $N1^{12/12}$; $N2^{21/21}$ double-homozygous mice, in which all N2ICD is expressed from the N1 locus.

(E and F) The levels of protein expressed from the N1 and N2 loci in developing RVs and SSBs were compared by immunostaining with N2ICD-specific antibodies on $N1^{12/12}$; $N2^{21/21}$ mice (the N1 locus; E) and WT (the N2 locus; F). The secondary antibody was used without signal amplification and exposure times were identical for the red channel to allow quantitative comparisons. Arrowhead denotes endothelial cells.

(G) Flow cytometry analysis on EGFP+ live cells from E13.5 Lfng-GFP kidneys with two different sets of anti-Notch ECD antibodies. All scale bars: 10 μm.

See also Figure S4.

cell-surface levels of N1 and N2 are comparable by flow cytometry, using LFng-GFP kidneys (Figure 2H). To minimize antibody-based artifacts, we employed two different sets of monoclonal anti-N1ECD and anti-N2ECD antibodies: one raised in Armenian hamster (Moriyama et al., 2008) and one raised in rat (Fiorini et al., 2009). The geometric mean fluorescence intensity (GMFI) of antibodies against N2 in EGFP+ epithelial cells isolated from E13.5 Lfng-GFP kidneys is ~4-fold (4.5 ± 1.0) higher than that generated by anti-N1 antibodies (Figure 4G). To ensure that this result did not reflect differential affinity, we sorted stable HEK293 cell lines in which surface biotinylation assays confirmed that the amounts of N1ECD and N2ECD on the cell surface were similar (described in the next section and in Figures S5A–S5C). The results show that the differences in affinity between N1 and N2 antibodies (Figure S5D) could account for only a fraction of the distribution difference seen in the RVs and SSBs. Therefore, N2 is more abundant than N1 on the surface of renal epithelial cells in the developing nephron. Most importantly, because N21 has the same surface abundance as N2 (Figure 2I), the ECD, but not the ICD, determines the surface level of N2 and N1.

N2ECD Releases More N1ICD than N1ECD Does in Response to Ligands

Considering that only one allele of *N2* is sufficient for normal kidney development, but two alleles of *N1* are not (Figure 3), a small difference in surface distribution alone may not explain the functional dominance of N2. Therefore, we asked whether differences in ECD composition could also impact the amount of ICDs released in response to ligand. To address this, we used a quantitative in vitro assay based on the LCI system in kidney-derived HEK293 cells (Figure 5A; Ilagan et al., 2011). We first fused the carboxy-terminal half of luciferase (CLuc) to the N terminus of RBP and generated two parental CLuc-RBP-expressing HEK293 Flp-In cell lines by random integration. Then we fused the N-terminal half of luciferase (NLuc) to the C terminus of full-length *N1* and *N21*, respectively, and targeted them into the same genomic locus in the two parental cell lines using the Flp-In system (Figure 5A). In these Notch Flp-In cells, the isogenic expression of N1-NLuc and N21-NLuc minimizes positional effects and ensures similar expression levels (Figures S5A–S5C). In the absence of ligand binding, N1-NLuc and N21-NLuc fusion proteins are anchored to the cell membrane, whereas CLuc-RBP fusion protein is segregated into the nucleus and no luciferase activity is detected. The binding of ligands to the ECD (or unfolding of the NRR by calcium chelation with EGTA) triggers receptor proteolysis and the release of the N1ICD-NLuc fragment, which then translocates into the nucleus and interacts with CLuc-RBP to reconstitute a quantifiable luciferase activity. The amount of light emitted is directly proportional to the amount of N1ICD released and is therefore a measure of signal strength (Ilagan et al., 2011). To control for cell-line specific variations, we tested a total of ten N1-NLuc subclones and ten N21-NLuc subclones for each of the two CLuc-RBP parental cell lines.

To compare the signal strengths of N1 and N21 in these cells, we cocultured the Notch Flp-In cells with either ligand-presenting cells (Chinese hamster ovary [CHO]-Dll1 or CHO-Jag1) or

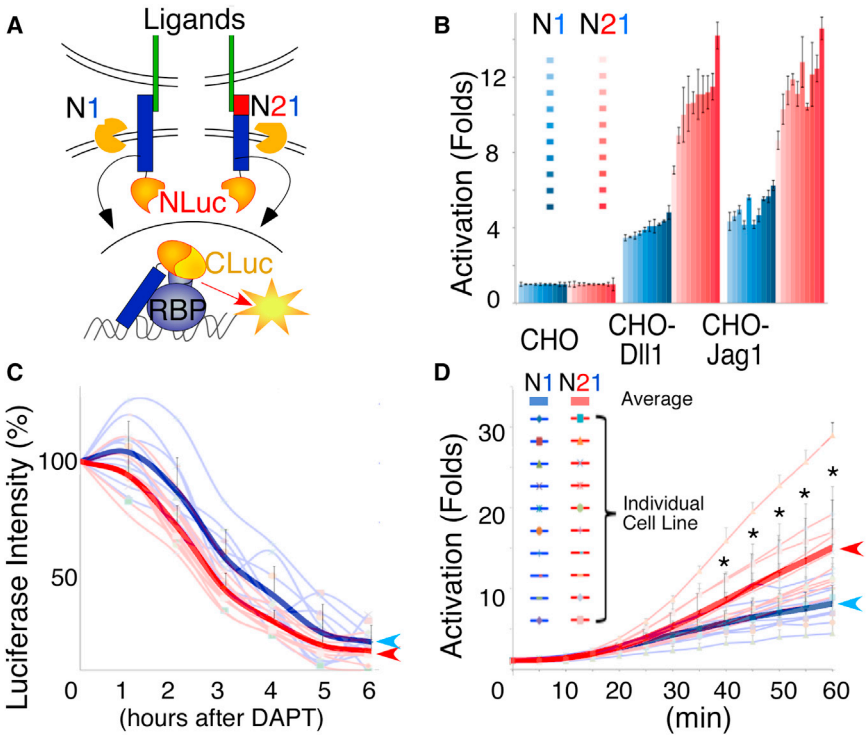

Figure 5. N2ECD Is More Potent than N1ECD in Mediating Ligand-Induced ICD Release

(A) The Notch LCI strategy for comparing the potency of N1ECD and N2ECD: NLuc is fused to the C terminus of N1 or N21. These two constructs were expressed from the same genomic locus in parental cell lines that stably express CLuc-RBP. For both N1 and N21, activation releases N1ICD-NLuc. The subsequent interaction of N1ICD-NLuc with CLuc-RBP reconstitutes luciferase. The amount of NICD released is proportional to the light produced.

(B and D) LCI results for ten independent cell lines in the presence of either (B) cocultured ligand-expressing cells (CHO-Dll1 and CHO-Jag1) or (D) 100 μM EGTA (*$p < 10^{-6}$, Student's t test).

(C) The stability of N1ICD-Nluc fragments released from N1 and N21 fusion proteins, which differ by six amino acids at the N terminus (VLLSRK and VIMAKR, respectively), was determined by the luminescence lifetime measurements after blocking NICD-NLuc release with the γ-secretase inhibitor DAPT. Thick lines in (C) and (D) represent the average of N1 and N21 cell lines. All scale bars represent SD.

See also Figure S5.

control CHO cells. After 24 hr of coculturing, significantly more light was emitted from N21-NLuc than from N1-NLuc cells ($p < 10^{-6}$, Student's t test; Figure 5B; similar results were obtained with subclones derived from the other CLuc-RBP-expressing parental cell line [not shown]). Considering that the released N1ICD-NLuc fragments from N21-NLuc and N1-NLuc differ by six amino acids at their N-termini (VLLSRK for N1-NLuc versus VIMAKR for N21-NLuc), we tested whether differential stability could account for the apparent difference in bioluminescence between N1-Nluc and N21-NLuc. After activating the reporter cells overnight on immobilized ligand, we added a γ-secretase inhibitor (DAPT) to block the release of additional N1ICD-NLuc fragments and followed the decay of bioluminescence as a function of time (Figure 5C). The N1ICD-NLuc^{VLLSRK} proved to be as stable as the N1ICD-NLuc^{VIMAKR}, allaying the concern that we were detecting differences in protein stability. Finally, as mentioned above, the amounts of N1 and N21 on the cell surface were similar (Figure S5), suggesting that the difference in luminescence is not simply due to unequal amounts of surface receptors. Collectively, these experiments suggest that N2ECD is more efficient in eliciting ligand-mediated receptor activation in kidney cells.

The activation of Notch receptors requires the unfolding of the NRR domain within the ECD to expose the S2 cleavage site (Kopan and Ilagan, 2009). We therefore tested whether differences in the dynamics of NRR unfolding might contribute to the differences between the two ECDs. We monitored the kinetics of N1 and N21 activation in our Flp-In lines in the presence of the calcium chelator EGTA for 1 hr. After 30 min of EGTA treatment, more bioluminescence was detected with N21-NLuc than with N1-NLuc (Figure 5D), suggesting that subtle differences in NRR unfolding may contribute to the higher activation probability of N21.

Dll1 and Jag1 Contribute Differentially to Nephron Segmentation

Two major Notch ligands, Dll1 and Jag1, are expressed in the developing renal epithelia (Chen and Al-Awqati, 2005; Leimeister et al., 2003). Coimmunostaining of SSBs shows that their expression domains largely overlap with each other (Figure 6A), with LFng (Figures 2E and 2G; Figure S3E), and with Notch receptors in the middle part of the SSBs (Figures 6B–6D). To assess the contribution of each ligand to nephron development, we created an allelic series of conditionally deleted ligands in the MM using *Six2-Cre^{tg}*/+ (Kobayashi et al., 2008; Figures 6E–6P). Because Six2-Cre is strongly expressed in MM cells from which all renal epithelial cells are derived, near-complete deletion of floxed Jag1 and Dll1 is achieved at the genomic DNA level in these cells (Figures S6A–S6D). Staining with the proximal tubule marker LTL revealed mildly disrupted nephron development in *Dll1* mutants (Figure 6H) but a drastic reduction in the number of nephrons in *Jag1* mutants (Figure 6J). Interestingly, in the presence of one *Jag1* allele (*Six2-Cre^{tg}*/+; *Dll1$^{f/f}$*; *Jag1$^{+/f}$*), nephron number was severely compromised, but some WT1+ podocytes formed (compare Figures 6N and 6M); the presence of one *Dll1* allele could not support production of podocytes, despite the presence of some proximal tubules (Figure 6O). Simultaneous deletion of both ligands led to a near-complete loss of nephrons (Figures 6L and 6P), approaching the drastic phenotype seen in N2 mutants in which both glomeruli and proximal tubules are missing (Cheng et al., 2007). These data collectively demonstrate that although both

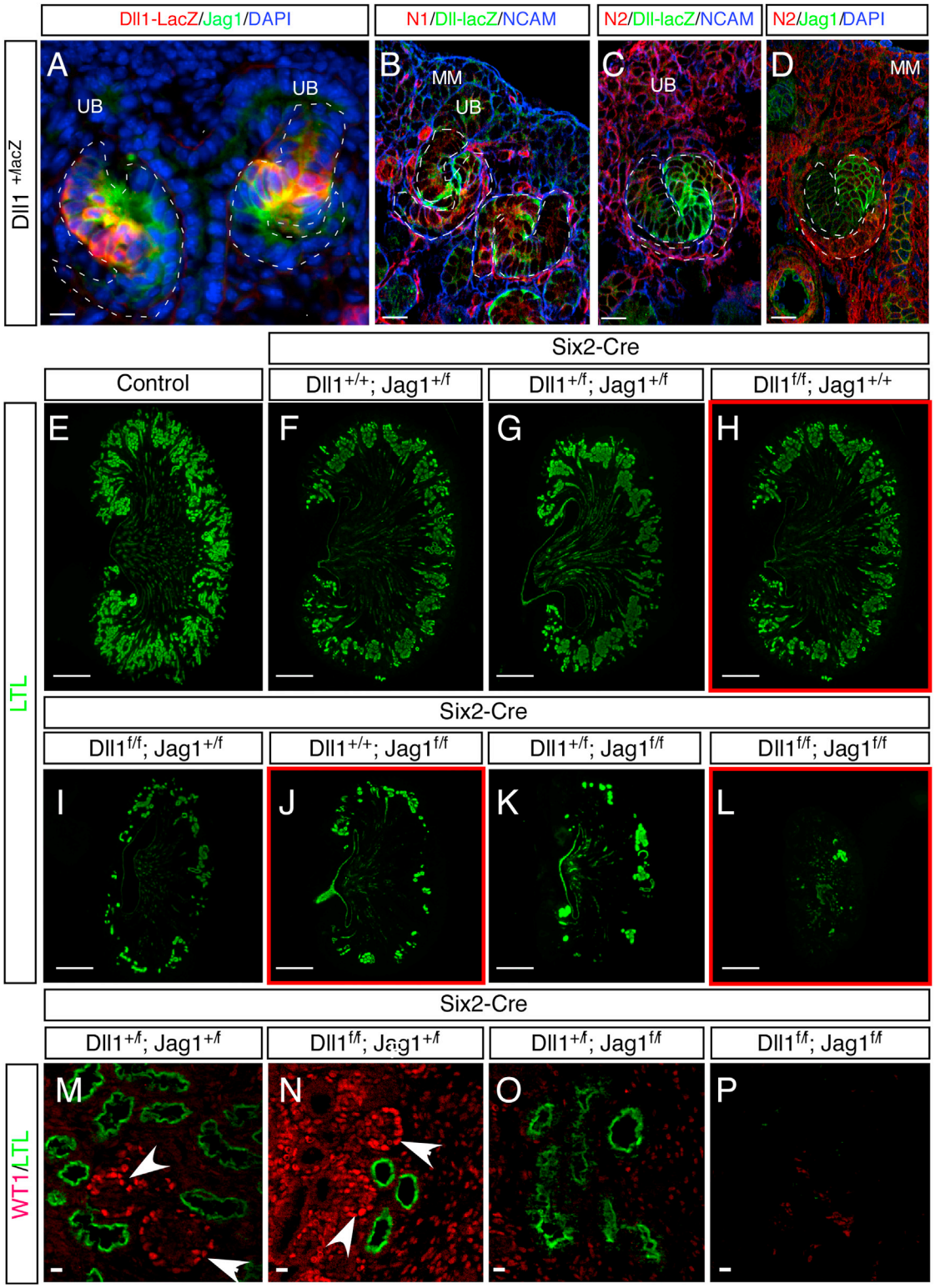

Figure 6. Jag1 Is the Dominant Ligand of N2 in the Kidney

(A–D) Comparison of N1, N2, Dll1, and Jag1 expression in the developing nephron.

(E–P) Phenotypes of newborn kidneys after ligand deletion. Scale bars: (A–D and M–P) 10 μm; (E–L) 500 μm.

See also Figure S6.

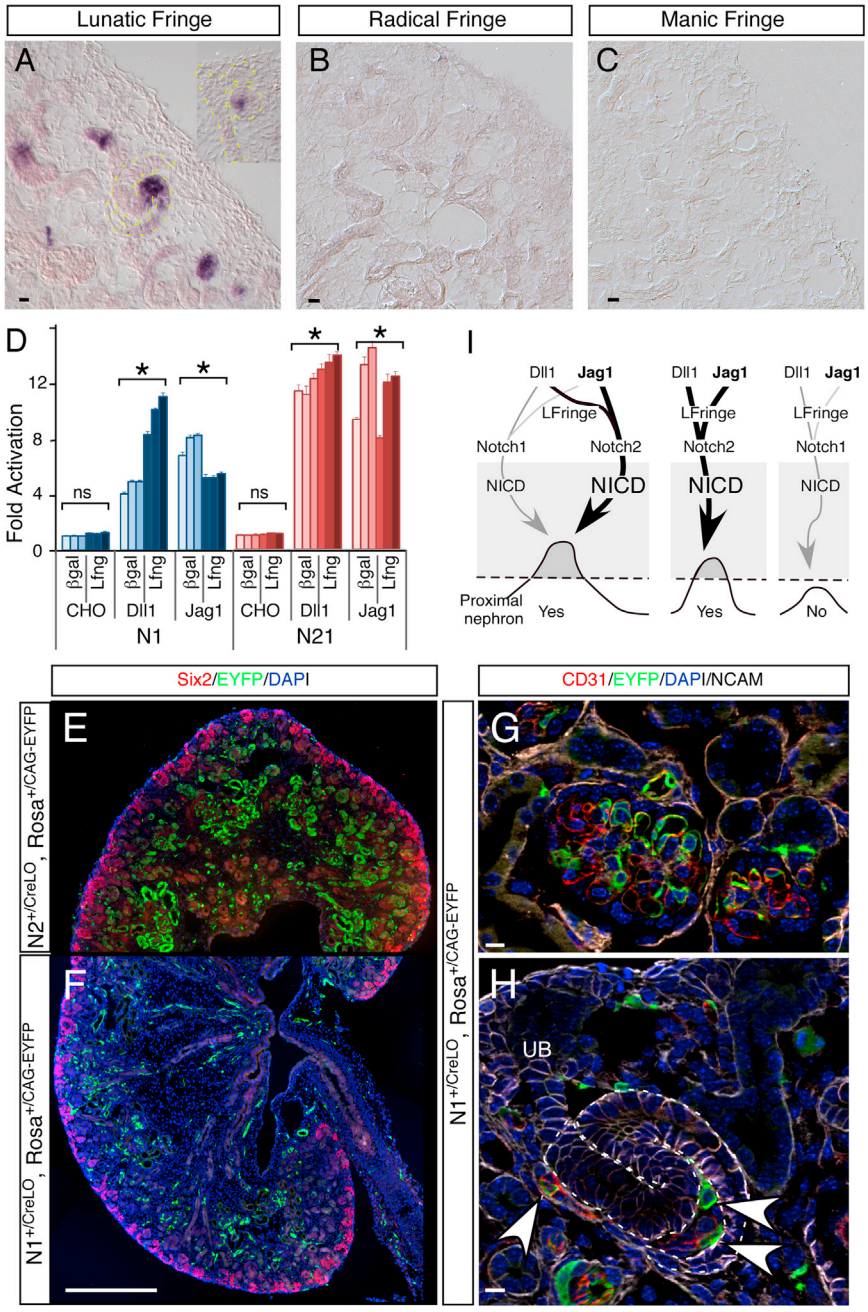

Figure 7. Modulation by Lfng Contributes to the Dominance of N2 in the Developing Kidney

(A–C) In situ hybridization of three fringe genes in the developing kidney. Inset in (A) shows an RV.

(D) Effects of Lfng modification on Notch1 and Notch21 activation in HEK293 cells (*$p < 0.05$, Student's t test). All scale bars represent SD.

(E–H) Comparison of the labeling pattern between N2::Cre^{LO} (E) and N1::Cre^{LO} (F–H) in vivo in developing nephrons. Arrowheads denote endothelial cells.

(I) A model proposing an NICD-dependent switch that regulates proximal nephron development and explaining how N2 achieves its dominant roles over N1. See Discussion for details. The weight of lines indicates the weight of effects. Scale bars: (A–C, G, and H) 10 μm; (E and F) 500 μm.

ligands contribute to the normal development of nephrons, Jag1 plays a dominant role in general and in the development of podocytes in particular.

Fringe family members can modulate the response of N1 and N2 to Dll1 and Jag1 ligands. In most contexts, fringe modification renders N1 more responsive to Dll1 ligand and less responsive to Jag1. In contrast, fringe modification of N2 can potentiate, reduce, or have no effect on ligand-mediated signaling, depending on the context (Stanley and Okajima, 2010). We therefore examined the expression pattern of the three fringe family members by in situ hybridization in E17.5 kidneys (Figures 7A–7C). We detected only Lfng, which was expressed in a pattern similar to that of EGFP from Lfng-GFP mice, with strong signal in some epithelial cells of RVs and the middle segment of SSBs, and weak signal in differentiated tubules (Figure 7A). We next compared the relative amounts of NICD released from N1-NLuc and N21-NLuc cell lines cocultured with Dll1- or Jag1-expressing CHO cells in the presence and absence of LFng. Overexpression of Lfng significantly enhanced the N1-NLuc response to Dll1 and suppressed its response to Jag1. In contrast, its effects on N21-NLuc were minimal (Figure 7D; only three lines of 20 are shown). Although the net loss in response to Jag1 may be offset by the gain in response to Dll1 in vitro (Figure 7D), these data suggest that fringe could contribute to the unequal contribution of N1 and N2 in vivo.

N2ECD Released Cre More Efficiently than N1ECD in Developing Nephrons of N::Cre mice

All of the data presented thus far ascribe the difference between N1 and N2 to their ECDs. Unfortunately, we have not yet identified antibodies that specifically recognize activated N2ICD. Therefore, we used a surrogate assay to compare N1 and N2 cleavage in vivo by comparing the effectiveness of Cre release in two activation-dependent Notch reporter mice: *N1::Cre^{Lo}* (Liu et al., 2011; Vooijs et al., 2007) and *N2::Cre^{Lo}* (Figure S1). The release of Cre in both lines is under the control of a Notch ECD, and Cre activity will provide an estimate of the efficiency of its release. Many labeled epithelial cells were seen in RVs and SSBs of *N2::Cre^{Lo}; Rosa$^{CAG-EYFP}$* mice (Figures 1M–1O and 7E). In contrast, we could not find any labeled epithelial cells in RVs or SSBs of *N1::Cre^{Lo}; Rosa$^{CAG-EYFP}$* mice, although endothelial cells are very efficiently labeled (Figures 7F–7H), as

are cells in many other tissues (Vooijs et al., 2007). Because we obtained immunohistological and genetic evidence that N1ICD complements N2 activity in a sensitized background (Cheng et al., 2007; Surendran et al., 2010), these observations are consistent with a model in which renal epithelia N2 is more abundant at the cell surface, where it undergoes proteolysis more efficiently than N1 in response to available ligands. Similar to the case with Notch ICDs, only Cre6MT released by N2ECD, but not N1ECD, reached the concentration threshold needed to excise the floxed stop allele in renal epithelial cells.

DISCUSSION

Results from human patients and mouse models of Alagille syndrome support the idea that kidney development is particularly sensitive to N2 dosage even in the presence of N1. We investigated several possible mechanisms that could explain the dominant contribution of N2 over N1 to nephrogenesis (Cheng et al., 2007; Surendran et al., 2010). A precise mechanistic understanding not only would enhance our knowledge of how Notch signaling contributes to kidney organogenesis but, more importantly, could also provide insights into therapeutic options for the kidney defects seen in Alagille syndrome (Penton et al., 2012) and perhaps other Notch-related congenital disorders. Furthermore, such an understanding could prove generally applicable to many other organs and signaling pathways.

Although N2 is expressed in the MM, none of the known Notch ligands or targets are expressed there (Boyle et al., 2011; Chen and Al-Awqati, 2005; Leimeister et al., 2003; Ong et al., 2006). Consistent with a ligand-poor environment, N2 activation is an infrequent event in the MM. Genetic analyses confirmed that Notch proteins function in nascent renal epithelial cells (this study; Cheng et al., 2007; Wang et al., 2003), where the *N1* and *N2* expression domains are indistinguishable (Chen and Al-Awqati, 2005; Leimeister et al., 2003). These results rule out enhancer evolution as the mechanistic explanation for the functional importance of N2.

We therefore focused on two alternative hypotheses: either N1ICD is a weak activator of key target(s) that are normally regulated by N2ICD due to its amino acid composition, or N1ICD concentration is insufficient to functionally compensate for N2 deficiency. To differentiate between these possibilities, we generated two alleles of Notch (*N12* and *N21*) in which we swapped the entire genomic sequences coding for Notch ICDs, in contrast to a previous study that established the equivalence of the domain C-terminal to the ankyrin repeats of Notch (Kraman and McCright, 2005). The availability of mice in which the same epitope is transcribed and translated from different loci enabled comparison of protein abundance with the same ICD-specific antibody. This analysis demonstrated that the two paralogs are expressed at similar levels in the developing renal epithelium, and therefore differences in overall protein concentration cannot explain the dominant role of N2.

We next addressed the role of Notch amino acid composition. We demonstrated that N1ICD and N2ICD are fully interchangeable during kidney development—even one copy of N1ICD expressed under the control of N2ECD is sufficient to produce a normal kidney. If neither the overall protein concentration nor the NICD composition can explain the unequal roles of N1 and N2 in the developing kidney, ECD control over NICD nuclear concentration is likely the differentiating factor between N2 and N1. We discovered that N2ECD indeed generates more NICD than N1ECD does in the renal epithelial cell context, by a combination of two mechanisms. First, N2 is more abundant at the cell surface than N1. Accounting for the differences in affinity between anti-N1 and anti-N2 antibodies, the difference is between 2- and 3-fold. Importantly, N21 and N2 are equally abundant at the cell surface, indicating that surface distribution is determined by sequences in the Notch ECD, not the ICD. Although other transmembrane proteins may contain trafficking signals in their ECD (Albu and Constantinescu, 2011; Steiner et al., 2008; Vanden-Bussche et al., 2009), the only indication that the Notch2 ECD may play a role in its trafficking comes from a study on the importance of S1 cleavage to the exocytosis of N1, but not N2 (Gordon et al., 2009). Second, in LCI assays (Ilagan et al., 2011) that quantified the amount of NICD released from N21 and N1 in cultured human embryonic kidney cells in response to ligand or EGTA, N21 consistently released more N1ICD. In the EGTA paradigm, all surface receptors are activated. Given that surface biotinylation confirmed that N1 and N21 are present at equal amounts, and the NICDs have the same half-life, we conclude that the N2 NRR must be easier to activate than N1 NRR in kidney epithelia, and since it contains the S1 site, it may regulate exocytosis as well. However, where the trafficking signals reside within the ECD, and whether they only function in the developing kidney, remains to be investigated. Supporting the conclusion that the ICD passively reflects the advantages provided by a specific ECD, N2ECD is more potent than N1ECD in Notch::Cre reporter mice, where the amount of Cre that is released directly reflects the activation frequency by the respective Notch ECD.

These two factors (surface density and ease of activation) may work in synergy or simply be additive, but other factors may serve to further amplify the effectiveness of N2ECD in vivo. As reported before (Hicks et al., 2000), the response of N1 to Jag1 is significantly inhibited by Lfng modification, whereas that of N2 is not. Considering that Lfng is coexpressed with N1 and N2 in the epithelial cells of developing nephrons, it may be promoting a potent N2-JAG1 signaling axis during nephrogenesis. Indeed, analysis of ligand loss-of-function alleles showed that, although Dll1 and Jag1 are coexpressed with N1 and N2, Jag1 plays a dominant role. This is consistent with reports that only mutations in *JAG1*, and not in *DLL1*, cause Alagille syndrome (Piccoli and Spinner, 2001).

The data presented here indicate that an NICD nuclear concentration threshold must be met to define the identity of the proximal renal epithelia, and this threshold acts as a digital (all-or-nothing) switch (Figure 7I). This is very reminiscent of the intestinal differentiation program in *Caenorhabditis elegans* (Raj et al., 2010). In that system, mRNA levels must rise above a threshold to activate expression of a master regulatory gene. The relative strength, or penetrance, of various alleles reflects the number of cells that reach the ON decision. In the Notch system, variability in the number of NICDs released to the nucleus may regulate an ON/OFF decision to form the proximal nephron. The advantage of N2ECD/NRR and the large impact of these differences suggest that the overall numbers of NICD in the nucleus are just above the ON state in RV cells and thus are highly prone to perturbations. Whether a master regulator lies downstream of

NICD and the identity/number of targets that must be activated to promote proximal development remain unknown.

In summary, our experiments have provided strong evidence for a functional equivalence between N1ICD and N2ICD in vivo, despite apparent differences in multiple assays based on overexpression, including our own (Ong et al., 2006). A higher surface level coupled with greater responsiveness of N2ECD to ligand translates into a higher probability of NICD release during a critical step in kidney development. These data illustrate the binary nature of a critical step in nephron segmentation, where nephrons with an NICD concentration below a certain threshold fail completely to produce proximal structures, and highlight an underappreciated importance for the ECD/NRR in controlling surface distribution. In contrast to binary response to NICD levels, the outcome of ligand reduction is graded: nephrons can form proximal tubules without podocytes when only Dll1 is present, suggestive of a second Notch-dependent decision. Finally, investigation into Notch paralogs trafficking to the cell surface may provide leads for treating the renal (and perhaps all) manifestations of Alagille syndrome.

EXPERIMENTAL PROCEDURES

Mice

Generation, genotyping strategy, and PCR primers related to N12 and N21 mice and the source of other mouse lines are described in detail in Supplemental Experimental Procedures. All mice were housed in the Washington University animal facility, and all experimental procedures were approved by the Washington University Animal Studies Committee.

Pyrosequencing

Total RNA was purified, reverse transcribed, and used for pyrosequencing as described previously (Liu et al., 2010).

Immunohistochemistry

Kidneys were dissected and fixed in 4% paraformaldehyde overnight, washed extensively with 1× PBS, soaked overnight in 30% sucrose, and embedded in optimal cutting temperature medium for frozen sections, or dehydrated through a 30%, 50%, 70% ethanol series and embedded for paraffin sections. For frozen sections, antigen retrieval was achieved by permeabilization in 1× PBS, 0.1% Triton X-100 for 20 min at room temperature. For paraffin sections, this was achieved by boiling in 10 mM sodium citrate (pH 6.0) for 20 min. For both frozen and paraffin sections, 1× PBS containing 3% BSA and 0.1% Tween was used for blocking. Detailed information on the primary antibodies and their dilution is provided in Supplemental Experimental Procedures. FITC-, Cy3-, and Cy5-conjugated secondary antibodies or streptavidin (Jackson ImmunoResearch) were used for visualization.

Flow Cytometry

Flow cytometry was performed as described previously (Liu et al., 2011). Briefly, E13.5 embryonic kidneys were dissected, mechanically disrupted, and digested with 1 mg/ml collagenase at 37°C for 15 min to obtain single-cell suspensions. Cells were further washed and stained with PE- or APC-conjugated anti-N1ECD or -N2ECD antibodies (eBioscience and Biolegend) in staining buffer (1× PBS +3% BSA) on ice for 20–30 min, followed by flow cytometry analysis. Cultured 293 cells were mechanically removed from culture plates and analyzed in a similar manner. Data were collected on a BD FACScan with FlowJo Collectors' Edition and analyzed with FlowJo software (TreeStar).

In Situ Hybridization, Western Blot, and Nephron Number Quantification

Conventional methods were used for in situ hybridization. Probes for lunatic, radical, and manic fringe were labeled with digoxigenin and detected with alkaline phosphatase-conjugated anti-digoxigenin antibody (Roche). Kidneys from newborn pups or cultured cells were used for western blotting. The number of nephrons was determined as previously described (Godley et al., 1996). Details are described in Supplemental Experimental Procedures.

Generation and Maintenance of Isogenic N1 and N21 LCI Reporter Lines

Flp-InTRex293 host cells (R780-07; Invitrogen), which were maintained in Dulbecco's modified Eagle's medium (DMEM) supplemented with 10% fetal bovine serum (FBS), 2 mM L-glutamine, 1% Pen-Strep (henceforth referred to as media), and 100 μg/ml Zeocin, were cotransfected with pcDNA3-(Click beetle green) CBG CLuc-RBP and a Puromycin expression construct using FuGENE6 (Roche). Puromycin-resistant clones were selected in media containing 0.6 μg/ml puromycin to generate Flp-InTRex 293 CBG CLuc-RBP parental cell lines. We performed LCI on CBG CLuc-RBP-expressing clones by transiently transfecting a constitutively active N1ΔE-NLuc plasmid to verify luciferase complementation. Two LCI-positive clones, D10 and D6, were selected as the CLuc-RBP parental cell lines and expanded in media containing 0.4 μg/ml puromycin and 100 μg/ml Zeocin. Stable expression of CLuc-RBP after different passages was confirmed by western blot. To generate N1-NLuc and N21-NLuc Flp-In cells, D10 and D6 clones were cotransfected with pcDNA5/FRT expression vector (V6010-20; Invitrogen) containing either N1-CBG NLuc or N21-CBG NLuc and pOG44 vector at a 1:9 ratio. Positive clones, identified by selection for hygromycin resistance (150 μg/ml) and gain of Zeocin sensitivity, were tested for their ability to reconstitute luciferase activity upon EGTA treatment. Subsequently, 20 subclones were maintained in media containing 0.4 μg/ml puromycin (to maintain CBG CLuc-RBP) and 100 μg/ml hygromycin (to maintain Notch CBG NLuc).

LCI Assays

LCI assays are described in detail in Ilagan et al. (2011). For ligand-dependent activation, 10^4 ligand-presenting cells (CHO-Dll, CHO-Jag, or CHO control cells) were seeded into each well of uncoated, 96-well black plates 24 hr prior to the seeding of 4×10^4 N1-NLuc or N21-NLuc cells. After another 24 hr, cocultured cells were imaged in phenol red-free culture medium containing 150 μg/ml D-luciferin. For the ligand-independent activation assays, 96-well black plates were coated with 0.1 mg/ml poly-lysine at room temperature overnight, washed twice with PBS, and air-dried for 30 min before 4×10^4 cells were seeded into each well. Twenty-four hours later, an initial image (t = 0) was obtained of the cells using Hank's balanced salt solution (HBSS) containing 150 μg/ml D-luciferin (100 μl/well). Then, another 100 μl of HBSS/D-luciferin solution containing 2× EGTA (200 μM) was added per well and images were obtained every 5 min for 1 hr.

To monitor the rate of NICD degradation, 96-well black plates were coated with 5 μg/ml anti-Fc antibody (Jackson ImmunoResearch) for 6 hr at 4°C. Unbound antibodies were washed off twice with PBS, and conditioned media containing Fc control or Dll1-Fc/Jag-Fc were added (50 μl/well) and incubated overnight at 4°C. Excess ligands were washed off twice with PBS before cells were seeded. Reporter cells were plated on the immobilized ligands as described previously (Ilagan et al., 2011). After 24 hr, an initial image was obtained (t = 0), after which DMSO or DAPT (5 μM) was added to the wells to stop NICD production, and images were taken every hour for 6 hr. Additional, detailed methods for ligand-conditioned media preparation, IVIS imaging, and photon flux quantification can be found in Ilagan et al. (2011).

Surface Biotinylation Assay

Surface biotinylation was used to compare the surface levels of N1-NLuc and N21-NLuc in Flp-In cells. Details are described in Supplemental Experimental Procedures.

SUPPLEMENTAL INFORMATION

Supplemental Information includes Supplemental Experimental Procedures and six figures and can be found with this article online at http://dx.doi.org/10.1016/j.devcel.2013.05.022.

ACKNOWLEDGMENTS

We thank the staffs of the Murine Embryonic Stem Cell Core, Mouse Genetics Core, and Siteman Flow Cytometry Core of the Siteman Cancer Center, Washington University, for their assistance. We thank Dr. MacDonald for providing unconjugated N1 and N2 antibodies, Dr. Groves for providing Lfng-GFP mice, and Dr. Blacklow for communicating unpublished results. We thank members of the Kopan laboratory for stimulating discussions and Mary Fulbright and Hila Barak for technical assistance. Z.L., S.C., S.B., A.Z., and R.K. were supported by the National Institute of Diabetes and Digestive and Kidney Disease (DK066408) and the National Institute of General Medicine (GM55479). M.X.G.I. and D.R.P.-W. were supported in part by the National Cancer Institute (CA094056).

Received: July 9, 2012
Revised: April 24, 2013
Accepted: May 23, 2013
Published: June 24, 2013

REFERENCES

Albu, R.I., and Constantinescu, S.N. (2011). Extracellular domain N-glycosylation controls human thrombopoietin receptor cell surface levels. Front. Endocrinol. (Lausanne) *2*, 71.

Boyle, S.C., Kim, M., Valerius, M.T., McMahon, A.P., and Kopan, R. (2011). Notch pathway activation can replace the requirement for Wnt4 and Wnt9b in mesenchymal-to-epithelial transition of nephron stem cells. Development *138*, 4245–4254.

Chen, L., and Al-Awqati, Q. (2005). Segmental expression of Notch and Hairy genes in nephrogenesis. Am. J. Physiol. Renal Physiol. *288*, F939–F952.

Cheng, H.T., Kim, M., Valerius, M.T., Surendran, K., Schuster-Gossler, K., Gossler, A., McMahon, A.P., and Kopan, R. (2007). Notch2, but not Notch1, is required for proximal fate acquisition in the mammalian nephron. Development *134*, 801–811.

Chu, D., Zhang, Z., Zhou, Y., Wang, W., Li, Y., Zhang, H., Dong, G., Zhao, Q., and Ji, G. (2011). Notch1 and Notch2 have opposite prognostic effects on patients with colorectal cancer. Ann. Oncol. *22*, 2440–2447.

Costantini, F., and Kopan, R. (2010). Patterning a complex organ: branching morphogenesis and nephron segmentation in kidney development. Dev. Cell *18*, 698–712.

Fan, X., Mikolaenko, I., Elhassan, I., Ni, X., Wang, Y., Ball, D., Brat, D.J., Perry, A., and Eberhart, C.G. (2004). Notch1 and notch2 have opposite effects on embryonal brain tumor growth. Cancer Res. *64*, 7787–7793.

Fiorini, E., Merck, E., Wilson, A., Ferrero, I., Jiang, W., Koch, U., Auderset, F., Laurenti, E., Tacchini-Cottier, F., Pierres, M., et al. (2009). Dynamic regulation of notch 1 and notch 2 surface expression during T cell development and activation revealed by novel monoclonal antibodies. J. Immunol. *183*, 7212–7222.

Fujimura, S., Jiang, Q., Kobayashi, C., and Nishinakamura, R. (2010). Notch2 activation in the embryonic kidney depletes nephron progenitors. J. Am. Soc. Nephrol. *21*, 803–810.

Georgas, K., Rumballe, B., Valerius, M.T., Chiu, H.S., Thiagarajan, R.D., Lesieur, E., Aronow, B.J., Brunskill, E.W., Combes, A.N., Tang, D., et al. (2009). Analysis of early nephron patterning reveals a role for distal RV proliferation in fusion to the ureteric tip via a cap mesenchyme-derived connecting segment. Dev. Biol. *332*, 273–286.

Godley, L.A., Kopp, J.B., Eckhaus, M., Paglino, J.J., Owens, J., and Varmus, H.E. (1996). Wild-type p53 transgenic mice exhibit altered differentiation of the ureteric bud and possess small kidneys. Genes Dev. *10*, 836–850.

Gordon, W.R., Vardar-Ulu, D., L'Heureux, S., Ashworth, T., Malecki, M.J., Sanchez-Irizarry, C., McArthur, D.G., Histen, G., Mitchell, J.L., Aster, J.C., and Blacklow, S.C. (2009). Effects of S1 cleavage on the structure, surface export, and signaling activity of human Notch1 and Notch2. PLoS ONE *4*, e6613.

Graziani, I., Eliasz, S., De Marco, M.A., Chen, Y., Pass, H.I., De May, R.M., Strack, P.R., Miele, L., and Bocchetta, M. (2008). Opposite effects of Notch-1 and Notch-2 on mesothelioma cell survival under hypoxia are exerted through the Akt pathway. Cancer Res. *68*, 9678–9685.

Hicks, C., Johnston, S.H., diSibio, G., Collazo, A., Vogt, T.F., and Weinmaster, G. (2000). Fringe differentially modulates Jagged1 and Delta1 signalling through Notch1 and Notch2. Nat. Cell Biol. *2*, 515–520.

Ilagan, M.X., Lim, S., Fulbright, M., Piwnica-Worms, D., and Kopan, R. (2011). Real-time imaging of notch activation with a luciferase complementation-based reporter. Sci. Signal. *4*, rs7.

Kobayashi, A., Valerius, M.T., Mugford, J.W., Carroll, T.J., Self, M., Oliver, G., and McMahon, A.P. (2008). Six2 defines and regulates a multipotent self-renewing nephron progenitor population throughout mammalian kidney development. Cell Stem Cell *3*, 169–181.

Kopan, R., and Ilagan, M.X. (2009). The canonical Notch signaling pathway: unfolding the activation mechanism. Cell *137*, 216–233.

Kraman, M., and McCright, B. (2005). Functional conservation of Notch1 and Notch2 intracellular domains. FASEB J. *19*, 1311–1313.

Leimeister, C., Schumacher, N., and Gessler, M. (2003). Expression of Notch pathway genes in the embryonic mouse metanephros suggests a role in proximal tubule development. Gene Expr. Patterns *3*, 595–598.

Liu, Z., Obenauf, A.C., Speicher, M.R., and Kopan, R. (2009). Rapid identification of homologous recombinants and determination of gene copy number with reference/query pyrosequencing (RQPS). Genome Res. *19*, 2081–2089.

Liu, Z., Schneider, D.L., Kornfeld, K., and Kopan, R. (2010). Simple copy number determination with reference query pyrosequencing (RQPS). Cold Spring Harb. Protoc. *2010*, pdb.prot5491.

Liu, Z., Turkoz, A., Jackson, E.N., Corbo, J.C., Engelbach, J.A., Garbow, J.R., Piwnica-Worms, D.R., and Kopan, R. (2011). Notch1 loss of heterozygosity causes vascular tumors and lethal hemorrhage in mice. J. Clin. Invest. *121*, 800–808.

Madisen, L., Zwingman, T.A., Sunkin, S.M., Oh, S.W., Zariwala, H.A., Gu, H., Ng, L.L., Palmiter, R.D., Hawrylycz, M.J., Jones, A.R., et al. (2010). A robust and high-throughput Cre reporting and characterization system for the whole mouse brain. Nat. Neurosci. *13*, 133–140.

McCright, B., Lozier, J., and Gridley, T. (2002). A mouse model of Alagille syndrome: Notch2 as a genetic modifier of Jag1 haploinsufficiency. Development *129*, 1075–1082.

Morimoto, M., Liu, Z., Cheng, H.T., Winters, N., Bader, D., and Kopan, R. (2010). Canonical Notch signaling in the developing lung is required for determination of arterial smooth muscle cells and selection of Clara versus ciliated cell fate. J. Cell Sci. *123*, 213–224.

Moriyama, Y., Sekine, C., Koyanagi, A., Koyama, N., Ogata, H., Chiba, S., Hirose, S., Okumura, K., and Yagita, H. (2008). Delta-like 1 is essential for the maintenance of marginal zone B cells in normal mice but not in autoimmune mice. Int. Immunol. *20*, 763–773.

Ong, C.T., Cheng, H.T., Chang, L.W., Ohtsuka, T., Kageyama, R., Stormo, G.D., and Kopan, R. (2006). Target selectivity of vertebrate notch proteins. Collaboration between discrete domains and CSL-binding site architecture determines activation probability. J. Biol. Chem. *281*, 5106–5119.

Parr, C., Watkins, G., and Jiang, W.G. (2004). The possible correlation of Notch-1 and Notch-2 with clinical outcome and tumour clinicopathological parameters in human breast cancer. Int. J. Mol. Med. *14*, 779–786.

Penton, A.L., Leonard, L.D., and Spinner, N.B. (2012). Notch signaling in human development and disease. Semin. Cell Dev. Biol. *23*, 450–457.

Piccoli, D.A., and Spinner, N.B. (2001). Alagille syndrome and the Jagged1 gene. Semin. Liver Dis. *21*, 525–534.

Raj, A., Rifkin, S.A., Andersen, E., and van Oudenaarden, A. (2010). Variability in gene expression underlies incomplete penetrance. Nature *463*, 913–918.

Rangarajan, A., Talora, C., Okuyama, R., Nicolas, M., Mammucari, C., Oh, H., Aster, J.C., Krishna, S., Metzger, D., Chambon, P., et al. (2001). Notch signaling is a direct determinant of keratinocyte growth arrest and entry into differentiation. EMBO J. *20*, 3427–3436.

Riccio, O., van Gijn, M.E., Bezdek, A.C., Pellegrinet, L., van Es, J.H., Zimber-Strobl, U., Strobl, L.J., Honjo, T., Clevers, H., and Radtke, F. (2008). Loss of intestinal crypt progenitor cells owing to inactivation of both Notch1 and

Notch2 is accompanied by derepression of CDK inhibitors p27Kip1 and p57Kip2. EMBO Rep. *9*, 377–383.

Rodríguez, C.I., Buchholz, F., Galloway, J., Sequerra, R., Kasper, J., Ayala, R., Stewart, A.F., and Dymecki, S.M. (2000). High-efficiency deleter mice show that FLPe is an alternative to Cre-loxP. Nat. Genet. *25*, 139–140.

Spitz, F., and Furlong, E.E. (2012). Transcription factors: from enhancer binding to developmental control. Nat. Rev. Genet. *13*, 613–626.

Stanley, P., and Okajima, T. (2010). Roles of glycosylation in Notch signaling. Curr. Top. Dev. Biol. *92*, 131–164.

Steiner, N.K., Dakshanamurthy, S., VandenBussche, C.J., and Hurley, C.K. (2008). Extracellular domain alterations impact surface expression of stimulatory natural killer cell receptor KIR2DS5. Immunogenetics *60*, 655–667.

Surendran, K., Boyle, S., Barak, H., Kim, M., Stomberski, C., McCright, B., and Kopan, R. (2010). The contribution of Notch1 to nephron segmentation in the developing kidney is revealed in a sensitized Notch2 background and can be augmented by reducing Mint dosage. Dev. Biol. *337*, 386–395.

VandenBussche, C.J., Mulrooney, T.J., Frazier, W.R., Dakshanamurthy, S., and Hurley, C.K. (2009). Dramatically reduced surface expression of NK cell receptor KIR2DS3 is attributed to multiple residues throughout the molecule. Genes Immun. *10*, 162–173.

Vooijs, M., Ong, C.T., Hadland, B., Huppert, S., Liu, Z., Korving, J., van den Born, M., Stappenbeck, T., Wu, Y., Clevers, H., and Kopan, R. (2007). Mapping the consequence of Notch1 proteolysis in vivo with NIP-CRE. Development *134*, 535–544.

Wang, P., Pereira, F.A., Beasley, D., and Zheng, H. (2003). Presenilins are required for the formation of comma- and S-shaped bodies during nephrogenesis. Development *130*, 5019–5029.

Warming, S., Costantino, N., Court, D.L., Jenkins, N.A., and Copeland, N.G. (2005). Simple and highly efficient BAC recombineering using galK selection. Nucleic Acids Res. *33*, e36.